Measuring pressure in equilibrium and nonequilibrium lattice-gas models

Mauro Sellitto

Dipartimento di Ingegneria, Università degli Studi della Campania "Luigi Vanvitelli", Via Roma 29, 81031 Aversa, Italy.

The Abdus Salam International Centre for Theoretical Physics, Strada Costiera 11, 34151 Trieste, Italy.[*]

(Dated: October 23, 2020)

Abstract

We develop an algorithm based on the method proposed by Dickman for directly measuring pressure in lattice gas models. The algorithm gives the possibility to access the equation of state with a single run by adding multiple ghost sites to the original system. This feature considerably improves calculations and makes the algorithm particularly efficient for systems with inhomogeneous density profiles, both in equilibrium and nonequilibrium steady states. We illustrate its broad applicability by considering some paradigmatic systems of statistical mechanics such as the lattice gas under gravity, nearest-neighbour exclusion models in finite dimension and on regular random graphs, and the boundary-driven simple symmetric exclusion process.

[*] mauro.sellitto@unicampania.it, mauro.sellitto@gmail.com

Pressure is a key thermodynamic parameter encoding the phase behaviour of macroscopic systems in thermal equilibrium [1]. As first realized by Tammann long ago [2, 3], for systems with many degrees of freedom the pressure behavior may not be as a simple as a mechanical interpretation would suggest. This is essentially due to the entropic contribution coming from the integral (or the sum) over the whole configuration space, which is at root of several unusual and conter-intuitive phenomena, such as inverse melting [4–6]. There is also a fundamental interest in extending the notion of pressure to active matter, a crucial step towards the formulation of a nonequilibrium statistical mechanics [7]. It is therefore of paramount importance to rely on flexible and viable algorithms that are capable of measuring the pressure directly, with no reference to a special state as in the standard thermodynamic integration method. This is all the more true for (athermal) lattice systems where Montecarlo algorithms are far less developed than their Molecular Dynamics counterpart [8, 9]. Previously proposed methods generally sacrifice the usual periodic boundary as they involve hard walls and volume fluctuations due to the removal or addition of a layer next to the wall [10]. We consider here an elegant solution proposed some time ago by Dickman in the context of lattice polymers [11, 12], which bears a strong resemblance with the ghost particle insertion trick suggested by Widom for computing the chemical potential [13]. The Dickman method consists of three simple yet important observations. First, for a lattice gas with volume V and Helmholtz free energy F, the pressure $P = -\partial F/\partial V$ is written as:

$$P = \lim_{\Delta V \to 0} \frac{k_{\mathrm{B}} T}{\Delta V} \ln \frac{Z(V + \Delta V)}{Z(V)} \,, \tag{1}$$

where Z is the canonical partition function. Then, one observes that the partition function of a system with volume V is equivalent to that of a modified system with volume $V + \Delta V$ in which one has added an infinite repulsive potential acting on the sites contained in ΔV (preventing particles from entering ΔV). Thus, if we introduce a repulsive potential of finite magnitude $U_\lambda = -k_{\mathrm{B}} T \ln \lambda$ acting on the sites in ΔV (in such a way that $\lambda = 0$ corresponds to $U = \infty$, and $\lambda = 1$ to $U = 0$), and denote with Z_λ the partition function of this modified system, we get $Z(V) \equiv Z_0(V + \Delta V)$ and $Z(V + \Delta V) \equiv Z_1(V + \Delta V)$, whence the partition function ratio in Eq. (1) becomes:

$$\ln \frac{Z_1(V + \Delta V)}{Z_0(V + \Delta V)} = \int_0^1 d\lambda \frac{\partial \ln Z_\lambda}{\partial \lambda} \,. \tag{2}$$

To transform this in something useful for the design of a Montecarlo algorithm, one finally

needs to remark that the partition function Z_λ for the modified system can be written as:

$$Z_\lambda(V+\Delta V) = \sum_{\Delta N=0}^{\Delta V} \lambda^{\Delta N}\Omega(N,\Delta N)\,, \tag{3}$$

where the summation is taken over the possible configurations of ΔN particles in ΔV and Ω is the total number of configurations with ΔN particles in ΔV and $N+\Delta N$ in $V+\Delta V$. Thus, the average number $\langle \Delta N\rangle$ of particles in ΔV can be obtained as:

$$\langle \Delta N\rangle = \lambda \frac{\partial \ln Z_\lambda}{\partial \lambda}\,. \tag{4}$$

This leads to the desired expression for the pressure:

$$P = \lim_{\Delta V\to 0} \frac{k_{\rm B}T}{\Delta V}\int_0^1 \langle \Delta N\rangle \frac{d\lambda}{\lambda}\,. \tag{5}$$

The pratical implementation of Eq. (5) in a Montecarlo algorithm obviously requires the interval of λ values be discretized, and numerical simulations carried out for different finite values of the repulsive potential. Also, the sites of ΔV on which the potential acts needs to be finite. To the best of our knowledge this is typically chosen to be as small as 1, and the single pressure-probe site is generally embedded in a wall of codimension 1 confining the system from one side. In this form it has been observed that the algorithm becomes problematic in the presence of a strong external bias, as in a lattice gas under gravity [14]. While, when dealing with pressures as tiny as those generated by the Casimir effect in a nonequilibrium driven system [15], the algorithm may require excessively long execution times, which is all the more troublesome for cooperative driven dynamics. Moreover, a naive extension of the algorithm allowing to probe the pressure at different locations, simultaneously, leads to unreliable results in nonequilibrium conditions.

We show in this paper that these drawbacks can be actually overcome, and that an efficient formulation of the algorithm can be consistently applied to a variety of physical situations of growing complexity, from a simple sedimentation problem to fluctuation-induced forces in a driven diffusive system. First of all, one should notice that some care is required when dealing with systems in which $\langle \Delta N\rangle \approx \Delta V$. In these cases there exists a limitation on the maximum value of pressure $P_{\rm max}$ that can be measured, as Eq. (4) diverges for $\lambda \to 0$, while $P_{\rm max} \approx -\log \lambda_{\rm min}$, (where $\lambda_{\rm min}$ is the minimum value of the λ discretization). Evidently, to correctly quantify the pressure when $\langle \Delta N\rangle \approx \Delta V$ one has to choose a suitable value of $\lambda_{\rm min}$. Second, it is important to emphasize that the presence of a confining wall is not a

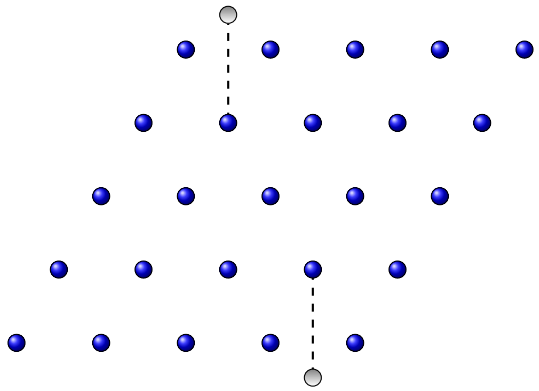

FIG. 1. Example of a portion of auxiliary system used for measuring pressure. A two-dimensional lattice of $V = 5 \times 5$ sites (represented as blue coloured balls), is augmented by two extra ghost sites (gray coloured balls, $\Delta V = 2$), which act as local pressure probes. Every ghost site increases by one the number of nearest neighbours of the lattice site to which it is linked (by a dashed line in the figure) and is subjected to a repulsive potential $U_\lambda = -k_\mathrm{B}T \ln \lambda$, but it does not participate to the nearest neighbour interactions of the lattice site to which it is linked. No wall is needed and boundary conditions can be periodic in any direction.

necessary ingredient for computing pressure in a Montecarlo simulation. If for some reason the spatial translational invariance of system geometry and interactions has to be preserved, one can use periodic boundary conditions (unless, of course, one is interested in the wall effects, as in wetting phenomena for example). Third, the size of ΔV can be relatively large, $\Delta V \gg 1$, provided that it is sub-extensive, $\Delta V \ll V$. This improves data statistics and becomes particularly relevant when the system under study displays an inhomogeneous density profile. In this case, multiple pressure probes distributed uniformly over the whole system can give access to the entire pressure profile with a single simulation run. Finally, once the wall is suppressed, it is important to specify how the (ghost) sites of ΔV are added to the original system. We do so by adding an extra nearest neighbouring site to a certain number, ΔV, of sites of the original system. In this way the local geometric structure of the original system is preserved and its intrinsic dynamics will be only weakly perturbed by the presence of these extra ghost sites (for a schematic representation, see Fig. 1). This point is particularly important as statistical mechanical models of interest generally involve static or dynamic spatially extended interactions.

In the following, the above points are implemented and carefully examined in systems for which the pressure has a purely entropic content, i.e., athermal systems. Comparison with theory is made whenever analytical results are partially or fully available. Montecarlo simulations are carried out in the grand canonical ensemble, in which the system of volume V (or one of its parts) is coupled to a reservoir R at chemical potential $\mu = \log[\rho_{\rm R}/(1-\rho_{\rm R})]$, where $\rho_{\rm R}$ is the reservoir density. Unless otherwise mentioned, the pressure-probe ghost sites are equally spaced in both the transverse and longitudinal directions of the system. At every Montecarlo time step, a lattice bond in the coupled system (ΔV + V + R) is randomly selected and, depending on the pair of sites involved, one of the three possibilities is considered: hole-particle exchange within the volume V, hole-particle exchange between V and the reservoir R, hole-particle exchange between V and the ghost volume ΔV. It is important to emphasize that the dynamics of the particle reservoir R is not explictly simulated. Rather, every time the randomly selected bond involves a site of R, its occupation state is randomly established by extracting a number with probabilty $\rho_{\rm R}$. The results we present were obtained by using the cut-off $\lambda_{\rm min} = 0.001$ and discretizing $\lambda \in [0,1]$ into 24 values equally spaced over three contiguous subintervals $[0.01, 0.04]$, $[0.04, 0.2]$ and $[0.2, 1]$, with steps $\Delta\lambda = 0.01,\ 0.02,\ 0.1$, respectively. Compared to a simple uniform discretization of $[0,1]$ this makes more effective the numerical evaluation of Eq. (5), because the contribution of smaller values of λ, which give a large contribution to the integral, is better weighted.

Lattice gas under gravity. To begin with, we discuss what is perhaps the simplest equilibrium system with a non-trivial inhomogeneous density profiles, the hard-core lattice gas under gravity. This provides a natural test bed for the algorithm as the system thermodynamics is simple enough to allow for a detailed comparison with the exactly known results. For a system of height $h_{\rm top}$ enclosed on the bottom and with the top in contact with a reservoir at density $\rho_{\rm top}$, the pressure at height h is given by:

$$P(h) = -k_{\rm B}T \log\left[1 - \rho(h)\right] , \tag{6}$$

where $\rho(h)$ is the density profile:

$$\rho(h) = \left\{1 + \frac{1-\rho_{\rm top}}{\rho_{\rm top}} \exp\left[\frac{m\,g}{k_{\rm B}T}(h - h_{\rm top})\right]\right\}^{-1} , \tag{7}$$

with mg being the gravity force. A further advantage of this problem is that the average

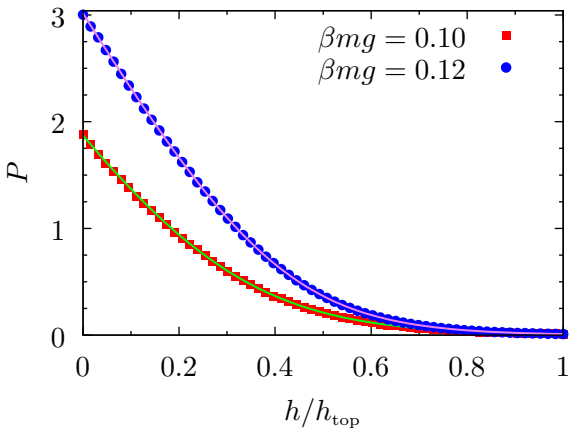

FIG. 2. Pressure p and particle density ρ vs height h in a tilted lattice gas under gravity. The system height is $h_{\rm top} = 64$ and base 64. The system top is in contact with a particle reservoir at density $\rho_{\rm top} = 0.01$. Periodic boundary condition in the direction normal to the gravity force. Full lines are the expected analytic results from Eqs. (6-7).

number $\langle \Delta N \rangle$ of particles in ΔV, Eq. (4), can be computed easily [14]:

$$\langle \Delta N(h) \rangle = \Delta V \frac{\lambda \rho(h)}{1 - \rho(h) + \lambda \rho(h)} \,, \tag{8}$$

providing a further detailed check of the algorithm. In the Montecarlo simulation we assume that boundary condition in the direction transverse to the gravity force is periodic and the ghost sites are uniformly distributed along the system diagonal. The square lattice is tilted by 45° and particle hopping is ruled by the standard Metropolis transition probability, $p = \min\{1, \exp(-\beta mg \Delta h)\}$, where $\Delta h = \pm 1$ is the height difference due to a single hop. In Fig. 2 we show the results for the density profile $P(h)$ for two different values of the gravity force, when the system top is kept in contact with a particle reservoir at density $\rho_{\rm top} = 0.01$. As we can see the analytic results are perfectly recovered [16]. In this form, the algorithm can be applied to more complex lattice models of colloidal sedimentation and granular compaction, like those of Refs. [17, 18].

Lattice gas with nearest neighbour exclusion. Next, we turn to a more interesting system of interacting particles, that is the lattice gas with nearest neighbour exclusion, where particles are forbidden to occupy the same or neighboring sites. This model has a long tradition in the study of critical phenomena as a schematic lattice model of hard-sphere

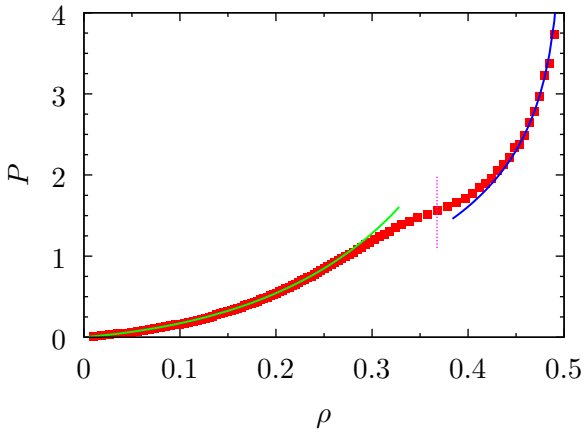

FIG. 3. Parametric plot of the equation of state, pressure $P = P(\mu)$ vs particle density $\rho = \rho(\mu)$, in a square lattice gas with nearest-neighbour exclusion. Full periodic boundary condition, system size $V = 32^2$ and ghost sites $\Delta V = 32$ located along the main diagonal of the lattice. The vertical dotted segment represents the analytic value of the critical density $\rho_c = 0.36774$. The full line below the critical density is a one-parameter fit obtained from the approach in Ref. [27] The full line at high-density is the non-interacting entropic pressure $-\log(1 - \rho/\rho_{\max})$ near the maximum packing density $\rho_{\max} = 1/2$.

fluids, and is closely related to the classical NP-hard combinatorial optimization problem of finding a minimum vertex cover on a random graph [19]. Numerical and theoretical studies for various finite dimensional lattices [20–27] have shown that there exists a critical density ρ_c (for a square lattice $\rho_c = 0.36774...$) at which the model exhibits a continuous phase transition to an ordered state with exponents that belong to the Ising universality class [25]. Above ρ_c particles tend to occupy preferentially one of the two sublattices in which the original lattice can be decomposed (in such a way that the nearest-neighbors of any sites of one sublattice belong to the other sublattice and vice-versa). The ground state, therefore, corresponds to a fully occupied sublattice and the maximum packing density is $\rho_{\max} = 1/2$. In Fig 3 we show the parametric plot of the equation of state $P(\rho)$ obtained in a grand-canonical simulation by slowly increasing the chemical potential. In agreement with the well establised numerical and theoretical results the equation of state displays an inflection point, corresponding to a divergent compressibility, near the critical density at which sublattice ordering occurs. The full line below the critical density is a one-parameter fit obtained from

the approach in Ref. [27], while the full line at higher densities is the non-interacting entropic pressure $-\log(1-\rho/\rho_{\max})$ near the closest packing density $\rho_{\max}=1/2$.

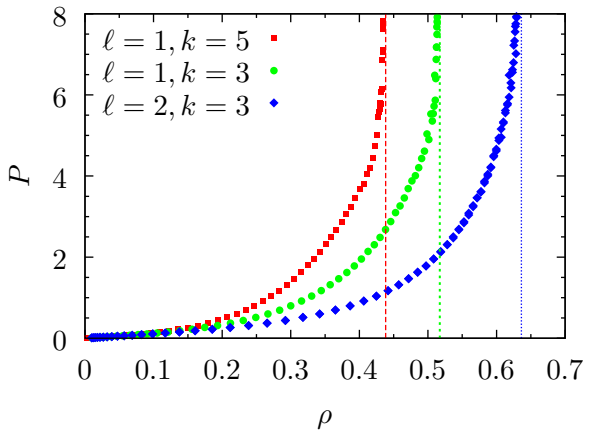

FIG. 4. Bethe lattice glass. Equation of state, pressure $P=P(\mu)$ vs particle density $\rho=\rho(\mu)$, in a parametric form, for a lattice gas on a regular random graph with connectivity $k+1$ and geometric constraint ℓ on particle occupation (every particle can have no more than ℓ particles as nearest neighbours). System size $V=2^{10}$, and ghost volume $\Delta V=2^5$ randomly located on the graph. Data points are the results of a Montecarlo simulation in the grand canonical ensemble in which the system is annealed by slowly increasing the chemical potential (starting from an empty system). Vertical lines correspond to the analytical values of the closest packing density obtained in Ref. [29].

Bethe lattice glass. The previously considered model can be interestingly generalised to situations in which every particle cannot have more than ℓ particles as nearest neighbours (thus, the nearest neighbour exclusion models is recovered for $\ell=0$). This class of models was introduced in the attempt of providing a microscopic finite-dimensional realization of the thermodynamic scenario for the elusive glass transition [28]. Subsequent works have shown that in finite dimension a freezing transition towards an ordered ground state occurs [30, 31]. However, some more sophisticated variants appears to be quite stable against crystalization and display properties of fragile glass-forming liquids [32, 33]. For the purpose of testing the present algorithm in a geometric structure other than the usual Euclidean lattices, we focus here on the monodisperse lattice glass model on the Bethe lattice. This is also known as regular random graph, that is locally tree-like geometric structure, with a fixed connectivity

$k+1$ and loops of order $\ln N$. This latter feature, an analog of generic boundary conditions, prevent unphysical surface effects and give arise to frustration precluding crystalline orderings. The resulting glassy behaviour can be studied analytically with the tools of disordered systems theory [28, 29], and has been extended to the quantum domain as well [34]. In Fig. 4 we show a parametric plot of the equation of state obtained in a grand canonical Montecarlo simulation for the Bethe lattice glass (with connectivity $k+1$ mimicking the square and cubic lattice) for two value of ℓ. Consistently with the analytical calculation[28], no sign of crystalization is observed in the equation of state and the pressure for large chemical potential tends to diverge at a density very near the closest packing limit, $\mu \to \infty$, obtained with the cavity method of disordered systems theory [29].

Fluctuation-induced force in a driven lattice gas. As a final more stringent test of the present algorithm we now consider a two dimensional system driven into a nonequilibrium steady state by two reservoirs at different densities, ρ_0 and ρ_1, located at its edges $x = 0$ and $x = L$, respectively. For such driven diffusive systems it is known that there exists long-range correlations [35], even for purely hard-core interactions [36]. A striking consequence is the appearance of Casimir-like forces in a finite geometry [15]. To the leading order in $\rho_1 - \rho_0$ and for a simple symmetric exclusion process [37] on a square lattice of size $L \times d$, this fluctuation-induced pressure, $\Pi(x)$, is given by [15]:

$$\Pi(x) = -\frac{1}{2Ld}\left[\frac{\rho_1-\rho_0}{1-\rho(x)}\right]^2 \frac{x}{L}\left(1-\frac{x}{L}\right) , \tag{9}$$

where $\rho(x) = \rho_0 + (\rho_1 - \rho_0)x/L$ is the system density profile and we set $k_{\rm B}T = 1$. For lattice system with only infinite hard-core repulsion the thermodynamic limit of the average density of particle, $\langle \rho_{\Delta \rm V} \rangle$, in the ghost volume ΔV is exactly known, see Eq (8). This means that the Casimir pressure, $\Pi_{\rm MC}(x)$, in a Montecarlo simulation with a finite ΔV can be measured as:

$$\Pi_{\rm MC}(x) \approx \int_0^1 \left[\langle \rho_{\Delta \rm V} \rangle - \frac{\lambda\rho(x)}{1-\rho(x)+\lambda\rho(x)}\right]\frac{d\lambda}{\lambda} . \tag{10}$$

where it is understood that the integral has to be properly discretized. In Fig. 4 we compare the Montecarlo results for $\Pi_{\rm MC}(x)$ at reservoirs densities $\rho_0 = 0.1$ and $\rho_1 = 0.7$ and different system sizes, with the theoretical result for $\Pi(x)$, Eq. (9), in the rescaled form $\widetilde{\Pi}(x) = L\,d\,\Pi(x)$. Data points of each curve were simultaneously obtained for a dynamical evolution long 10^9 Montecarlo sweeps, and averaged over a sample of 10 to 20 elements (statistical

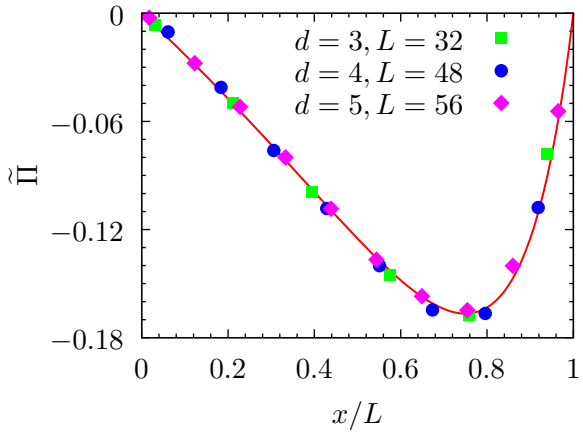

FIG. 5. Fluctuation-induced pressure profile $\widetilde{\Pi}(x) = L\, d\, \Pi(x)$ in the simple symmetric exclusion process on a square lattice of size $d \times L$. The system edges at $x = 0$ and $x = L$ are in contact with boundary reservoirs at density $\rho_0 = 0.1$ and $\rho_1 = 0.7$, respectively. There are periodic boundary condition in the direction transverse to the particle current, and the number of ghost sites is $\Delta V = 2d$ (so that $\Delta V/V = 2/L$). Red line refers to Eq. (9).

errors are not visible because of the order of symbol size). The agreement is excellent and fully confirms the efficiency and functionality of our algorithm.

In conclusion, we have developed an algorithm based on the Dickman which can considerably improve the accuracy of Monte Carlo calculations of pressure in lattice models, and is especially suited for systems with inhomogeneous density profiles, both in equilibrium and nonequilibrium steady states. The algorithm is quite general and holds the key to many other statistical mechanics applications.

Acknowldgements. I gratefully acknowledge Daniel Martin and José Luis Iguain for valuable suggestions in the early stage of this work. I also thank Avi Aminov, Jef Arenzon and Yariv Kafri for kindly clarifying some aspects of their work [15, 27]. Numerical simulations were performed by using ICTP computer facilities.

Data Availability. The data that support the findings of this study are available from

the corresponding author upon reasonable request.

---

[1] H.B. Callen, *Thermodynamics and an Introduction to Thermostatistics*, (J. Wiley & Sons, New York 1985).

[2] G. Tammann, *Kristallisieren und Schmelzen*, (Johann Ambrosius Barth, Leipzig, 1903), pp. 26–46.

[3] A.L. Greer, Nature **404**, 134 (2000).

[4] S. Rastogi, G.W.H. Höhne, and A. Keller, Macromolecules **32**, 8897 (1999).

[5] F.H. Stillinger and P.G. Debenedetti, Biophys. Chem. **105**, 211 (2003).

[6] N. Schupper and N. M. Shnerb, Phys. Rev. E **72**, 046107 (2005).

[7] A.P. Solon, Y. Fily, A. Baskaran, M. E. Cates, Y. Kafri, M. Kardar, J. Tailleur, Nature Physics **11**, 673 (2015).

[8] D. Frenkel and B. Smit, *Understanding molecular simulation: from algorithms to applications*, (Elsevier, 2001).

[9] W. Krauth, *Statistical Mechanics: Algorithms and Computations*, (Oxford University Press, Oxford 2006).

[10] P. Pendzig, W. Dieterich, and A. Nitzan, J. Chem. Phys. **106**, 3703 (1997).

[11] R. Dickman, J. Chem. Phys. **87**, 2246 (1987).

[12] For a review, see: R. Dickman in: *Numerical Methods for Polymeric Systems*, S.G. Whittington ed. (Springer, New York 1998).

[13] B. Widom, J. Chem. Phys. **38**, 2808 (1963).

[14] D.C. Hong, K. McGouldrick, Physica A **255**, 415 (1998).

[15] A. Aminov, Y. Kafri, and M. Kardar, Phys. Rev. Lett. **114**, 230602 (2015).

[16] Notice that for values of βmg larger that those we used the bottom layers become densely occupied, $\langle \Delta N \rangle \approx \Delta V$, and pressure is correctly measured only if a suitable value of $\lambda_{\min}$ is properly chosen.

[17] Y. Levin, J.J. Arenzon and M. Sellitto, Europhys. Lett. **55** 767-773 (2001).

[18] J.J. Arenzon, Y. Levin and M. Sellitto, Physica A **325**, 371 (2003).

[19] M. Hartmann and M. Weigt, *Phase transitions in combinatorial optimization problems* (Wiley: New Jersey 2006).

[20] D.S. Gaunt and M.E. Fisher, J. Chem. Phys. **43**, 2840 (1965).

[21] F.H. Ree and D.A. Chesnut, J. Chem. Phys. **45**, 3983 (1966)

[22] L.K. Runnels and L.L. Combs, J. Chem. Phys. **45**, 2482 (1966).

[23] D.S. Gaunt, M.E. Fisher, J. Chem. Phys. **46**, 3237 (1967).

[24] R.J. Baxter, I.G. Enting, and S.K. Tsang, J. Stat. Phys. **22**, 465 (1980).

[25] W. Guo and H.W.J. Blöte, Phys. Rev. E **66**, 46140 (2002).

[26] H.C.M. Fernandes, Y. Levin, and J.J. Arenzon, J. Chem. Phys. **126**, 114508 (2007).

[27] H.C.M. Fernandes, Y. Levin, and J.J. Arenzon, Phys. Rev. E **75**, 052101 (2007).

[28] G. Biroli and M. Mézard, Phys. Rev. Lett. **88**, 025501 (2001).

[29] O. Rivoire, G. Biroli, O.C. Martin, and M. Mézard , *Eur. Phys. J. B* **37**, 55 (2004).

[30] K.A. Dawson, S. Franz, and M. Sellitto, Europhysics Letters (EPL) **64**, 302 (2003).

[31] E. Marinari and V. Van Kerrebroeck, Europhysics Letters (EPL) **73**, 383 (2005).

[32] R.K. Darst, D.R. Reichman, and G. Biroli, J. Chem. Phys. **132**, 044510 (2010).

[33] Y. Nishikawa and K. Hukushima, arXiv:2003.02872v2 (2020).

[34] L. Foini, G. Semerjian, and F. Zamponi, Phys. Rev. B **83**, 094513 (2011).

[35] For a review, see: J.R. Dorfman, T.R. Kirkpatrick and J.V. Sengers, Annu. Rev. Phys. Chem. **45**, 213 (1994).

[36] H. Spohn, J. Phys. A **16**, 4275 (1983).

[37] For a review, see: B. Derrida, J. Stat. Mech. (2007) P07023.